A Modular Multilevel Converter with Integrated Self-balancing Series IGBTs

Lu Yue
Department of Electrical Engineering
State University of New York at Buffalo
Buffalo, USA
luyue@buffalo.edu

Xiu Yao
Department of Electrical Engineering
State University of New York at Buffalo
Buffalo, USA
xiuyao@buffalo.edu

***Abstract*—Modular multilevel converters (MMC) and series-connected IGBTs are two promising solutions to high-voltage dc (HVDC) transmission. It has been shown that, when integrated with series IGBTs, a MMC can benefit from a reduced number of sub-modules (SMs), simpler control, and improved reliability. In this paper, a MMC prototype, with the capability to integrate series IGBTs to replace single IGBTs in the sub-modules, is designed and developed. The MMC control is realized with a real-time simulator for versatile software implementation. The voltage sharing among the series IGBTs is regulated locally without the intervention of the central control. Furthermore, voltage balance under bi-directional current through the series strings is achieved. Experiments were conducted where individual IGBTs in one sub-module were replaced with a series of three IGBTs each. The results verify that the MMC is functional since the local series IGBT control and the MMC central control are independent. It is also verified that both series strings can maintain voltage balance at the same time even though the string currents shift directions.**

I. Introduction

Ever since its introduction, Modular Multilevel Converters (MMCs) have been a promising solution to the ever-increasing voltage demand from high-voltage dc (HVDC) [1]. A MMC excels at reaching a high output voltage simply by stacking more sub-modules because of its modular design. There has been extensive study on the topology of the MMCs and control methods, such as SM capacitor voltage balancing control (VBC) and circulating current suppression control (CCSC) [2]–[8]. However, compared to the abundant literature on modeling and the control of the MMCs, there has been less research focusing on the hardware development of MMCs [9]–[14]. Most prototypes proposed in current research are rated at less than 500 V per SM. One advantage of low-voltage designs is that numerous SMs can be fitted under a lower source voltage. However, it should be addressed that with increased voltage rating, the size of the SM capacitors increases, PCB design becomes more challenging, and IGBTs may display different switching characteristics.

Additionally, with a higher number of SMs, size and cost of the MMC also rise. Furthermore, the control scheme becomes more complicated and additional controllers can be used to control groups of SMs instead of single ones [9]. If one IGBT is faulty, the entire SM is decommissioned [15], reducing the reliability. Consequently, there must be backup SMs. Alternatively, research has been done to combine MMCs with series IGBTs to reduce the number of SMs [16], [17]. In this case, if one IGBT fails, the other IGBTs in the same string will take its share of voltage. Therefore, the SM will stay online. Furthermore, the utilization of series IGBTs in MMCs offers benefits such as a decreased number of SMs, and thus a smaller physical size. The control of a MMC will also simplify once the number of SMs reduces, especially if the series IGBTs do not drain extra resources from the central controller.

However, the series IGBTs need voltage balancing control, otherwise the voltage sharing among IGBTs will be imbalanced, causing device failure [18]. A wide range of study has been published on the topic of series IGBT voltage balancing. Consequently, numerous methods have been proposed, ranging from using passive snubber circuits or voltage clamps [19]–[22] to using advanced digital control to ensure that the transient balance is closely monitored and guided [23]–[25]. However, when scrutinized against the requirements for implementation in more advanced topologies to replace individual switching devices, such as the IGBTs in a MMC, most voltage balancing methods are unfit. This inadequacy can be attributed to two factors. First, the MMC control itself can be complicated. Therefore, it is desirable that the series IGBT balancing control does not introduce extra computation load on the central controller. Second, more crucially, when used in advanced topologies, the series IGBTs may need to conduct current flow that is bi-directional. In general, series IGBT voltage balancing under reverse current flow, from emitter to collector, is under-studied.

To address the above-mentioned issues, a MMC prototype is proposed in this paper. The system structure and sub-module design are presented. Then, a modified MMC control is proposed, allowing the integration of series IGBTs. The voltage balancing method in [26] and [27] was implemented since the balancing method does not require a central controller. It was further developed to gain the ability to balance series IGBT voltages with bi-directional currents. Afterwards, single IGBTs of one SM were replaced with series IGBTs strings augmented with proposed voltage balancing control. Finally, experimental results are presented to demonstrate that the two series strings can achieve voltage balance with changing currents, while the MMC operates normally.

978-1-7281-4829-8/20/$31.00 ©2020 IEEE

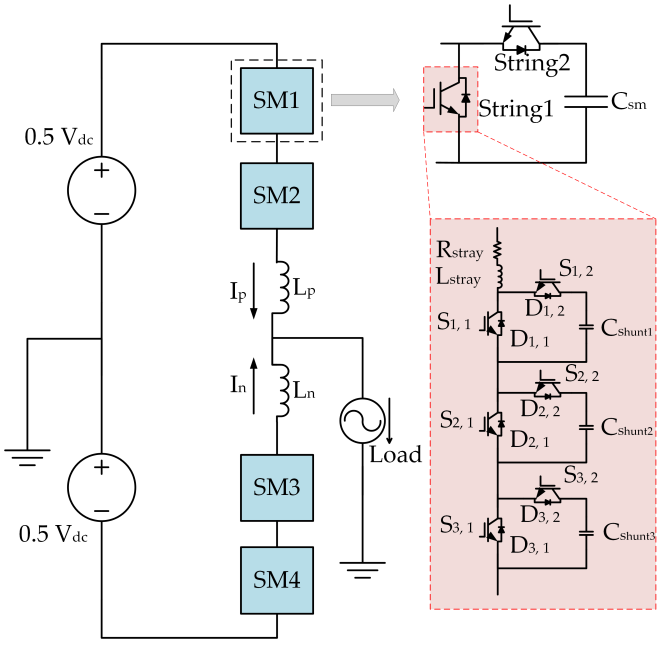

Figure 1: Circuit topology of the MMC with one series-IGBT SM.

II. Modular Multilevel Converter System and Hardware Design

A. MMC System Design

The circuit topology of the MMC is shown in Fig. 1. For this paper, a single-phase MMC with two SMs per arm was designed and built. Later, one of the SMs will be replaced with two series IGBT strings. The system design is shown in Fig. 2. Major groups include two arms, communication boards serving as the interfaces for optical and electrical signals, and the controllers for capacitor voltage balancing, circulating current suppression, and PI control, etc.

The central control is realized with a real-time simulator OP4510, whose operation can be modified and monitored on a PC with Simulink. When the scale of the MMC is small enough with fewer than 14 SMs in total, the real-time simulator can serve both as central and arm controllers. Otherwise, dedicated arm controllers are needed. If OP4510 servers as both the central and the arm controller, critical MMC operation information is measured and transmitted to the controller via BNC cables. After processing the data, IGBT gate signals are fed to the communication board from the central controller and delivered to the corresponding gate drivers. With dedicated arm controllers, V_{Csm} balancing and individual SM control duties will be released from the central controller to the arm controllers, while PI control and circulating current suppression will still be executed in the central controller.

B. Sub-module Design

The block diagram of one sub-module is given in Fig. 3. The optical interface is used to control the ADC, which senses both SM capacitor voltage and arm current and transfers the data output. The optical interface is also used to receive gate signals from the controllers. The analog interface transmits analog voltage and current signals back to the central controller for PI control, circulating current suppression control, and V_{Csm} balancing. Since the SM operates on a floating ground determined by the status of other SMs, galvanic isolation must be ensured between the quantities being measured and the analog interface. As a result, isolation amplifier-based sensing circuits are used with an insulation rating of 5 kV. The SM capacitors are connected externally, so that the circuit boards can be compact and less susceptible to EMI. Both the SM PCB and the SM capacitors are mounted onto two aluminum plates serving as buses. With such a configuration, the C_{sm} value becomes variable as one can conveniently add or remove capacitors. A small bypass capacitor is placed on the PCB parallel to C_{sm}, offering a low inductance return path for the high frequency noise during transients. Fig. 4 provides a photograph of the assembled MMC prototype.

III. MMC Integration of Series-IGBT Sub-module

A. Closed-Loop MMC Control

The simplified control diagram for the MMC is shown in Fig. 5. Both load current and circulating currents are derived from the arm currents.

Proportional-resonance controllers are used to extract the harmonics from the circulating current to generate V_{adj}, which

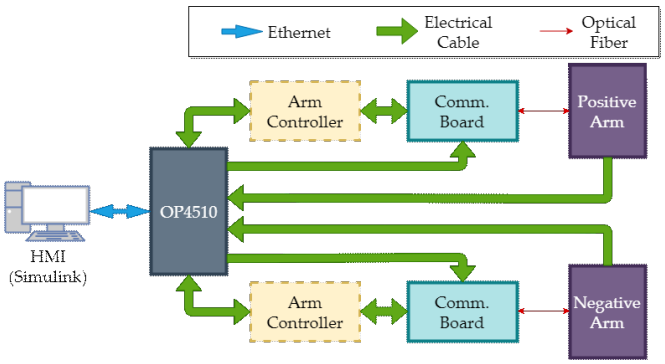

Figure 2: System block diagram of proposed MMC.

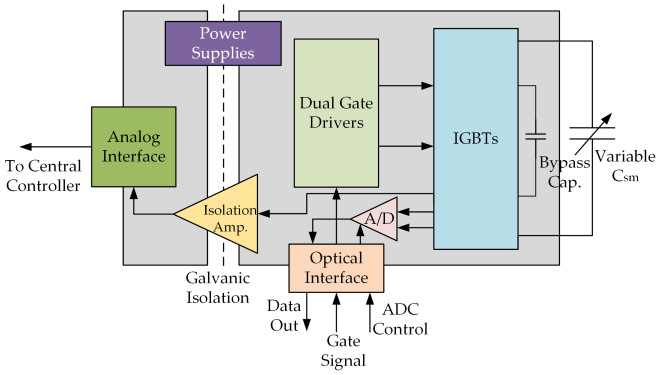

Figure 3: System block diagram of one sub-module.

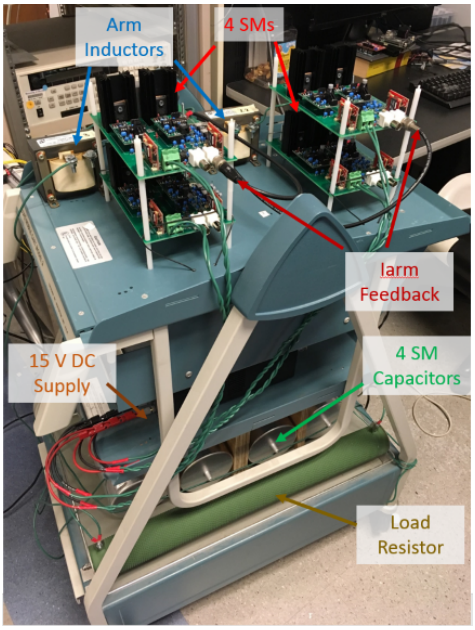

Figure 4: The MMC setup with 2 SMs per arm.

will then be subtracted from the reference signals. The adjusted references are modulated to compute the number of SMs to turn on or off for the next cycle. The Voltage Balancing Control (VBC) determines which SM will act based on the ranking of the V_{Csm} as well as the current direction of that arm. Finally, VBC's decisions are sent to each SM for execution.

B. Modified MMC Control to Integrate Series IGBT SM

For the series IGBTs, the self-balancing control has been presented and discussed in detail in [26] and [27]. To provide an overview for the following analysis, the balancing method can be summarized as follows.

To regulate the voltage sharing among the series IGBTs with the help of the auxiliary circuits in Fig. 1, intentional gate delays are assigned to each series module. If the gate delays are generated in such a way that a capacitor with a lower voltage will get charged more or discharged less, the capacitor voltage will increase. One way to generate such delays, without the need for a central controller or high-speed digital components, is through the biasing of a common triangular carrier based on the V_{Cshunt} feedback. As shown in Fig. 7a, the carrier Tri+ corresponds to a series module whose share of voltage is higher than a virtual set point, represented by Tri in the middle. The resulting main IGBT

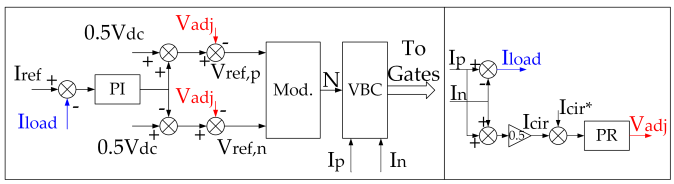

Figure 5: Simplified MMC control diagram.

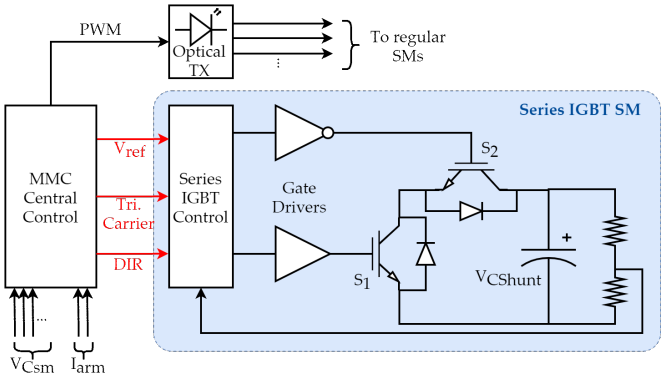

Figure 6: Modified control method to integrate self-balancing series IGBTs.

gate pulse for the Tri+ module is then wider than what would result from Tri. Since the shunt capacitors get inserted into the circuit complementary to the main IGBTs, the shunt capacitor for Tri+ module will be inserted for a shorter amount of time. Assuming the current through the series branch is in the direction to charge the shunt capacitors, the Tri+ shunt capacitor will then get charged less, leading to a decrease in voltage.

When integrated into a MMC, the current through a series string is not always from collectors to emitters. Rather, determined by the status of other sub-modules, the current can be bi-directional, which imposes a challenge to the voltage balancing among IGBTs. Fortunately, the self-balancing method, with modifications, can achieve voltage balance with bi-directional currents.

When the current through the IGBTs is "negative", i.e. from emitters to collectors, and if a series module has a higher V_{CShunt}, the corresponding triangular carrier should be subtracted by an amount that is determined by the feedback signal. From the blue Tri- waveform in Fig. 7a, it can be

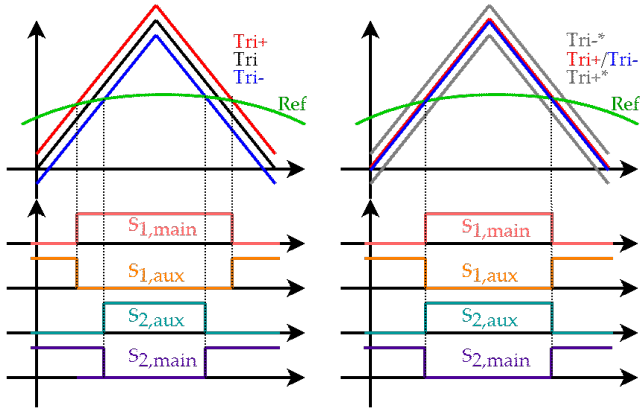

(a) No Bias results in large overlap and dead-time. (b) With Bias, the gate pulses are better aligned.

Figure 7: Comparison of PWM with and without the *Bias* term in the control equations.

deduced that the resulting main IGBT gate pulse is narrower than the set point. It then follows that the corresponding shunt capacitor will be inserted for a longer time relative to the others. Consequently, if the current is "negative", the capacitor will be discharged more and its voltage will fall. Therefore, to integrate the self-balancing IGBTs in a MMC, the direction of the string current must be considered since it determines which control rule to follow. The DIR input in Fig. 6 fulfills the above-mentioned role. The DIR can be either from the MMC central control or from a local current sensor within the series string. However, directly applying the positive or negative biases to the triangular carriers may likely cause issues for the half-bridge configuration.

C. Implementation of Voltage Balancing Control for Bi-directional Current

From the previous discussion, the triangular carrier biasing rules can be simply written as follows.

$$Tri_{out} = \begin{cases} Tri_{comm} + V_{C,fb1};\ \text{DIR = 1} \\ Tri_{comm} - V_{C,fb2};\ \text{DIR = 0} \end{cases} \quad (1)$$

where Tri_{comm} is the unbiased carrier and $V_{C,fb}$ is the capacitor voltage feedback signal.

When Eq. 1 is used on series IGBTs on the same string or on strings with the same current direction, the resulting Tri_{out} differ from each other by $\Delta V_{C,fb}$, usually a small bias to generate a delay of a few micro-seconds. However, in a half-bridge setup, the two strings can have different DIR values. Furthermore, the $V_{C,fb}$ signals will most likely contain a dc offset, because adaptiveness dictates that they need to be able to reflect the actual V_{Cshunt} over a wide range. Therefore, when one string's carriers are shifted upwards while the other string's carriers are shifted downwards, long delays are introduced to the PWM signals. One case is illustrated in Fig. 7a, in which Tri+ and Tri- are the carriers of two strings with different DIRs. As a result, both strings' main IGBTs stay ON significantly longer than before, creating cross-conductions between them, as shown by the overlap between $S_{1,main}$ and $S_{2,main}$ in Fig. 7a. On the other hand, the auxiliary IGBTs from both strings will have a prolonged dead-time, resulting in more severe dead-time effects [28].

One way to modify Eq. 1 to mitigate the above-mentioned problem is by introducing a $Bias$ term to both equations, as shown below.

$$Tri_{out} = \begin{cases} Tri_{comm} + V_{C,fb1} - Bias;\ \text{DIR = 1} \\ Tri_{comm} - V_{C,fb2} + Bias;\ \text{DIR = 0} \end{cases} \quad (2)$$

The triangular carriers in Fig. 7a become shifted, as shown in Fig. 7b. The virtual set point, Tri+*, that generated Tri+ is now shifted downwards while Tri-* is shifted upwards. The results are that the actual triangular carriers, Tri+ and Tri-, are much closer, and the gate pulses do not suffer from overlap or overly long dead-times. When one series module is compared with another from the same string, the bias in the carriers stays

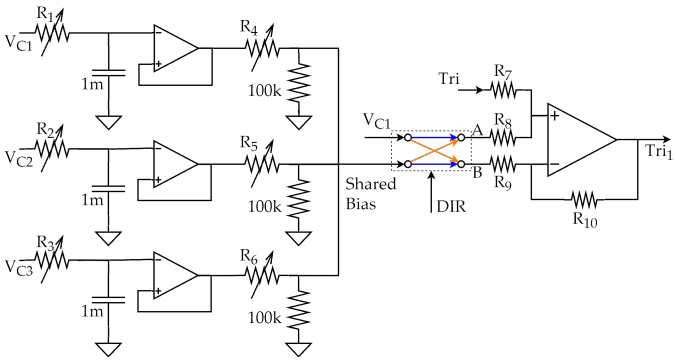

Figure 8: The controller circuit diagram with shared $Bias$ and DIR selector.

the same, $\Delta V_{C,fb}$. However, when the same series module is compared with its counterpart from the other string with a different DIR, the triangular carrier bias becomes $2V_{C,fb} - 2Bias$. If $Bias$ stays close to $V_{C,fb}$, the delays between two strings become negligible.

One method to synthesize such $Bias$ signal is shown in Fig. 8. The dc components of $V_{Cshunt1}$ to $V_{Cshunt3}$ are extracted via a low-pass filter network and their average value is obtained if R4, R5, and R6 are zero. The average value, shared by all the series modules without the intervention of a central controller, is the $Bias$ signal. This method offers two advantages: first, the $Bias$ is relatively close to all the V_{Cshunt} in the string; second, if group voltage varies, $Bias$ will also vary accordingly without the need for re-tuning. Therefore, the $Bias$ signal provides good safety, as well as adaptability.

The next stage of implementation involves realization of Eq. 2. It can be seen that Tri_{out} follows the format of $Tri_{comm} + A - B$, and that based on different DIRs, A and B are either $V_{C,fb}$ or $Bias$, respectively. Two analog switches can be used to realize this action of selecting. The following stage is for the computation to complete using an operational amplifier. The final output stage sees the generation of PWM signals by modulating a common reference with the biased triangular carriers. The IGBT gate signals will contain the voltage balancing information.

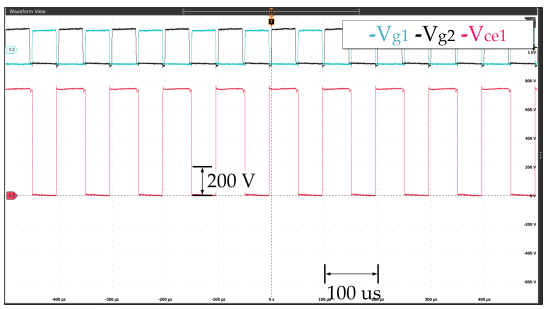

Figure 9: Single sub-module test result at 750 V.

IV. Experimental Verification

For this section, all the data used to construct the figures was gathered with a MSO58 oscilloscope with additional chan-

nels from a DPO5054B oscilloscope, except Fig. 12, which was recorded from OP4510's ADC channels. The voltages were measured with THDP0200 probes while the currents were measured with TCP202A probes. The dc supply was a Keysight N8925A with 750 V maximum voltage. The OP4510 real-time simulator ran at a fixed time step of 50 micro-second.

A. Regular MMC Operation

First, the individual sub-modules are tested to confirm that they can handle 750 V. The test result of one SM is shown in Fig. 9. It can be seen that the SM is able to handle 750 V safely with little switching noise.

Then, open-loop operation was tested with 750 V dc source voltage at 1 kHz switching frequency. Other parameters are given in Table I. The results in Fig. 10 show that the MMC operates normally with open-loop control. Since the modulation method is N+1 PWM, where N = 2, the output demonstrates three levels: 0, $0.5V_{dc}$, and V_{dc}.

Table I: Circuit parameters

Parameter	Value	Parameter	Value
V_{dc}	750 V	C_{sm}	1 mF
L_p/L_n	1 mH	C_{shunt}	1 uF
R_{load}	220 Ohm	f_{sw}	375 V
L_{load}	100 mH		

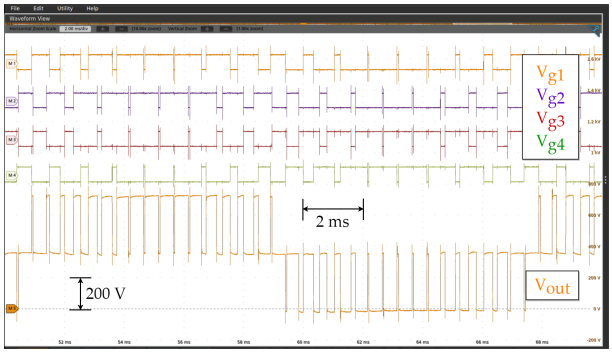

Figure 10: Gate signals and the output of the MMC with open-loop control.

The closed-loop results, shown in Fig. 11, demonstrate similar multiple voltage levels at the output: 0, $0.5V_{dc}$, and V_{dc}. However, the $0.5V_{dc}$ level is noisier than that from the open-loop. This is caused by the lack of V_{Csm} balancing control. With open-loop control, all C_{sm} are given approximately the same chance to charge or discharge. Contrarily, with closed-loop control, errors are introduced, which then translate to uneven switchings, increasing the V_{Csm} imbalance. However, as will be demonstrated in the next subsection, even if the MMC does not have a circulating current control or SM voltage balancing control, the series IGBT voltage balance can still be achieved since the proposed control method is independent of MMC system-level controls. The voltage sharing control requires the MMC to provide steady arm currents to charge or discharge shunt capacitors during injected delays, regardless of how much circulating current is found in the arm currents.

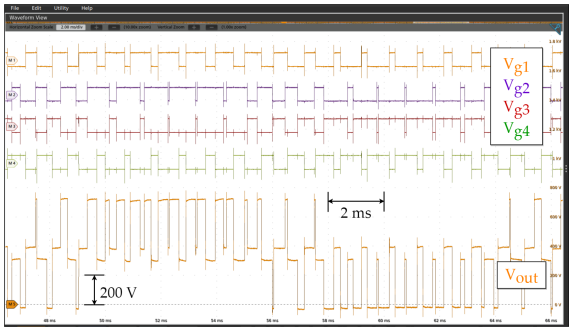

Figure 11: Gate signals and the output of the MMC with closed-loop control.

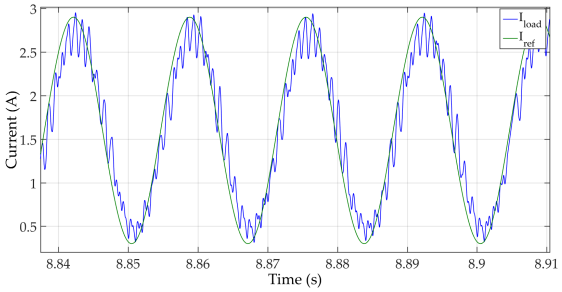

Figure 12: Load current follows the reference current during closed-loop operation.

In the real-time simulator, which serves as the controller, load current is monitored and compared with the reference current, as shown in Fig. 12. One can see that the load current follows the reference current closely.

B. Self-balancing Controller Verification

As illustrated in Fig. 7b, when the current direction changes, two strings' triangular carriers must stay close to each other to avoid prolonged overlap or dead-time between the gate pulses. Therefore, it is imperative to examine and ensure that the controllers meet the requirement. As shown in Fig. 13, when DIR of String1, which corresponds to the lower switch in a half-bridge, flips from 0 to 1, the minor voltage difference between the carriers of each string remained the same in magnitude but with simply a different sign.

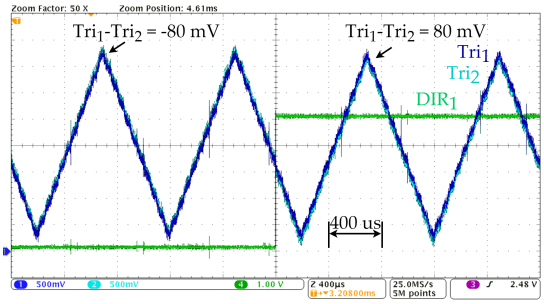

Figure 13: Triangular carriers of two strings with DIR1 changes from 0 to 1.

When Tri1 and Tri2 from Fig. 13 are used to modulate the same reference signal, the delay can be calculated as follows.

$$\Delta t = \frac{\Delta V_{tri}}{2 f_{sw} V_{tri,max}} = 10\ \mu s \tag{3}$$

The delay is around 1% of one switching cycle, which is safe given that the dead-time is approximately 2% to 3% of one cycle. Given a fixed ΔV_{tri}, the resulted Δt can be further tuned by changing the magnitude of the carrier, or by changing the carrier shape, such as to a trapezoid.

C. MMC Operation with Series-IGBT SM

For the series-IGBT SM test, the voltage per SM is limited at 100 V for component and PCB safety considerations since each series module is rated at 100 V. In Fig. 14, the voltage sharing of both strings is shown for one fundamental cycle. For the series IGBT tests, the MMC source voltage is 450 V with the series IGBT module sharing around 230 V. Therefore, when balanced, each series module withstands approximately 75 V.

On the one hand, for String1, balanced voltage sharing is maintained throughout the cycle, with the biggest voltage imbalance peaks around 4 V briefly. On the other hand, V_{ce4} to V_{ce6} in String2 are well-balanced in the beginning and the end of the cycle, while they temporarily lose balance in the middle due to noise in the circuit. The imbalance occurring after the disturbance is around 11 V maximum. However, as shown in Fig. 14, within 6 switching cycles after the disturbance, balance is regained and maintained. It is also worth mentioning that the process of regaining balance on String2 after the disturbance spans a current direction change on both strings. The fact that the voltage balancing proceeds through such a transition verifies its effectiveness and safety.

An example of the controllers' balancing effort is demonstrated in Fig. 15. Over the four cycles, it can be seen that the voltage sharing on String2 recovers from a disturbance to balance. The zoomed-in window shows that the two series modules with lower voltages, V_{ce4} and V_{ce6}, are given longer delays to charge their capacitors and thus, a voltage rise. It can also be seen that since V_{ce4} and V_{ce6} are nearly the same, they are given almost the same delays at turn-off.

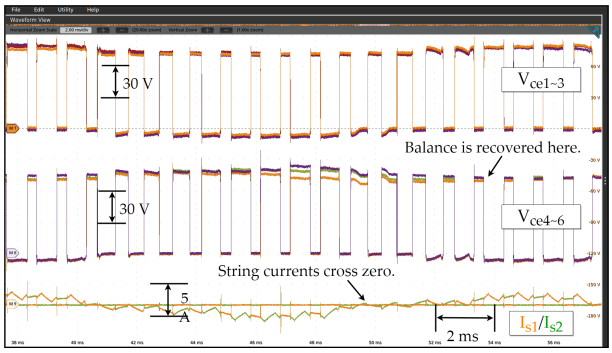

Figure 14: The voltage sharing of both strings with bi-direction currents.

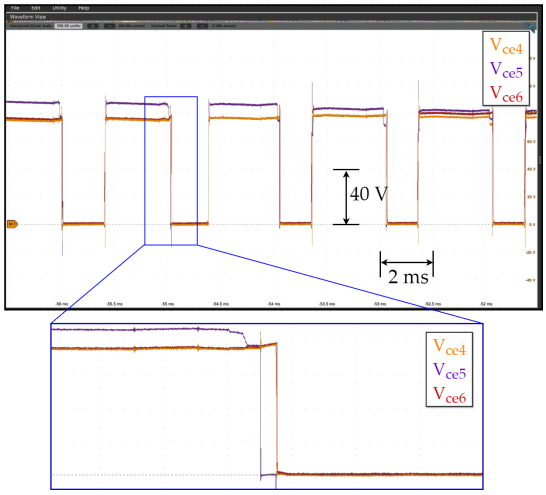

Figure 15: The recovery process from a disturbance with zoomed-in window showing controller effort.

With the series IGBT sub-module replacing a regular one, the MMC output voltage and current are presented in Fig. 16. The output voltage contains three levels: 0, $0.5V_{dc}$, and V_{dc}. The current is a 60 Hz sinusoidal with ripples limited by the load inductor. Similar to the output voltage in Fig. 11, there exists a band around $0.5V_{dc}$, caused by the imbalances among V_{Csm}. One can see that, on the system level, the MMC operates similarly with and without the series IGBT SM.

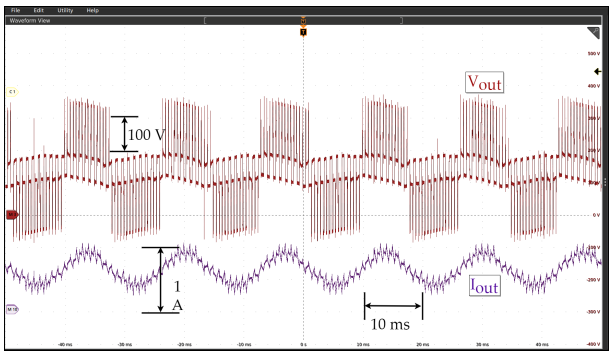

Figure 16: MMC output voltage and current with series IGBTs integrated.

V. Conclusion

In this paper, a MMC prototype is presented, including its topology, system structure, and SM design. The MMC can be solely controlled by a real-time simulator, or with additional controllers. The control method for the prototype was also illustrated with modifications to integrate series IGBTs to replace single IGBTs. The series IGBTs are locally controlled to achieve a balanced voltage sharing with bi-directional current flow. Experimental results were presented showing that single SMs can handle 750 V and that the MMC can operate with both open and closed loop at 750 V. Furthermore, the series IGBT strings in one sub-module are capable of maintaining balanced voltage sharing at the same time even if the current

changes directions. In the future, additional features will be added to the prototype to enable V_{Csm} balance and circulation current suppression.

ACKNOWLEDGMENT

This material is based upon work supported by the National Science Foundation under grant no. ECCS 1711659.

REFERENCES

[1] A. Lesnicar and R. Marquardt, "An innovative modular multilevel converter topology suitable for a wide power range," in *Proc. IEEE Power Tech. Conf.*, Bologna, Italy, 2003.

[2] G. Son, H. Lee, T. Nam, Y. Chung, U. Lee, S. Baek, K. Hur, and J. Park, "Design and control of a modular multilevel hvdc converter with redundant power modules for noninterruptible energy transfer," *IEEE Transactions on Power Delivery*, vol. 27, no. 3, pp. 1611–1619, 2012.

[3] W. Do, S. Kim, T. Kim, and R. Kim, "A study of circulating current in mmc based hvdc system under an unbalanced grid condition," *Transactions of the Korean Institute of Electrical Engineers*, vol. 64, no. 8, pp. 1193 – 1201, 2015.

[4] J. Moon, J. Kim, Cand Park, D. Kang, and J. Kim, "Circulating current control in mmc under the unbalanced voltage," *IEEE Transactions on Power Delivery*, vol. 28, no. 3, pp. 1952 – 1959, 2013.

[5] S. Li, X. Wang, Z. Yao, and Z. Li, T Peng, "Circulating current suppressing strategy for mmc-hvdc based on nonideal proportional resonant controllers under unbalanced grid conditions," *IEEE Transactions on Power Electronics*, vol. 30, no. 1, pp. 387 – 397, 2015.

[6] M. Glinka and R. Marquardt, "A new ac/ac multilevel converter family," *IEEE Transactions on Industrial Electronics*, vol. 52, no. 3, pp. 662 – 669, June, 2005.

[7] S. Rohner, S. Bernet, and R. Hiller, M Sommer, "Modulation, losses, and semiconductor requirements of modular multilevel converters," *IEEE Transactions on Industrial Electronics*, vol. 57, no. 8, pp. 2633 – 2642, 2010.

[8] Q. Tu, Z. Xu, and L. Xu, "Reduced switching-frequency modulation and circulating current suppression for modular multilevel converters," *IEEE Transactions on Power Delivery*, vol. 26, no. 3, pp. 2009 – 2017, 2011.

[9] Y. Zhou, D. Jiang, P. Hu, J. Guo, Y. Liang, and Z. Lin, "A prototype of modular multilevel converters," *IEEE Transactions on Power Electronics*, vol. 29, no. 7, pp. 3267 – 3278, Aug. 2013.

[10] L. Bessegato, A. Narula, P. Bakas, and S. Norrga, "Design of a modular multilevel converter prototype for research purposes," in *Proc. IEEE 2018 20th European Conference on Power Electronics and Applications (EPE'18 ECCE Europe)*, Riga, Latvia, 2018.

[11] B. Li, D. Xu, D. Xu, and R. Yang, "Prototype design and experimental verification of modular multilevel converter based back-to-back system," in *Proc. IEEE 2014 IEEE 23rd International Symposium on Industrial Electronics (ISIE)*, Istanbul, Turkey, 2014, pp. 626–630.

[12] M. Moranchel, F. M. Sanchez, E. J. Bueno, F. J. Rodriguez, and I. Sanz, "Six-level modular multilevel converter prototype with centralized hardware platform controller," in *Proc. IEEE IECON 2015 - 41st Annual Conference of the IEEE Industrial Electronics Society*, Yokohama, Japan, 2015, pp. 3863 – 3868.

[13] S. Zhang, S. Wang, N. Praisuwanna, L. Kong, R. Martin, F. Wang, and L. M. Tolbert, "Development of a flexible modular multilevel converter test-bed," in *Proc. IEEE 2018 IEEE Energy Conversion Congress and Exposition (ECCE)*, Oregon, USA, 2018, pp. 5250 – 5257.

[14] J. Kolb, F. Kammerer, and M. Braun, "Dimensioning and design of a modular multilevel converter for drive applications," in *Proc. IEEE 2012 15th International Power Electronics and Motion Control Conference (EPE/PEMC)*, Novi Sad, Serbia, 2012.

[15] E. Solas, G. Abad, J. A. Barrena, S. Aurtenetxea, A. Carcar, and L. Zajac, "Modular multilevel converter with different submodule concepts—part i: capacitor voltage balancing method," *IEEE Transactions on Industrial Electronics*, vol. 60, no. 10, pp. 4525 – 4535, 2013.

[16] L. Yue and X. Yao, "Investigation of control and applications of modular multilevel converter with sub-modular series igbts," in *2018 IEEE Applied Power Electronics Conference and Exposition (APEC)*, San Antonio, TX, USA, 2018, pp. 1486–1491.

[17] B. Jacobsson, P. Karlsson, G. Asplund, L. Harnefors, and T. Jonsson, "Vsc - hvdc transmission with cascaded two-level converters," in *Conseil International des Grands Réseaux Électriques (CIGRE)*, Paris, France, 2010.

[18] J. Baek, D. Yoo, and H. Kim, "High-voltage switch using seriesconnected igbts with simple auxiliary circuit," *IEEE Transactions on Industry Applications*, vol. 37, no. 6, pp. 1832 – 1839, 2001.

[19] J. Chen, J. Lin, and T. Ai, "The techniques of the serial and paralleled igbts," in *Proc. IEEE 22nd International Conference on Industrial Electronics, Control, and Instrumentation*, Taipei, Taiwan, 1996, pp. 999 – 1004.

[20] X. Chen, L. Yu, T. Jiang, H. Tian, K. Huang, and J. Wang, "A fast and series-stacked igbt switch with balanced voltage sharing for pulsed power applications," *IEEE Transactions on Plasma Science*, vol. 45, pp. 2328–2334, Aug. 2017.

[21] J. H. Kim, B. D. Min, S. V. Shenderey, and G. H. Rim, "High voltage pulsed power supply using igbt stacks," *IEEE Transactions on Dielectrics and Electrical Insulation*, vol. 14, pp. 921–926, Aug. 2007.

[22] M. Zarghani, S. Mohsenzade, and S. Kaboli, "A fast and series-stacked igbt switch with balanced voltage sharing for pulsed power applications," *IEEE Transactions on Plasma Science*, vol. 44, pp. 2013 – 2021, Oct. 2016.

[23] T. C. Lim, B. W. Williams, S. J. Finney, and P. R. Palmer, "Series-connected igbts using active voltage control technique," *IEEE Transactions on Power Electronics*, vol. 28, no. 8, pp. 4083–4103, Aug. 2013.

[24] T. Lu, Z. Zhao, J. Shiqi, H. Yu, and L. Yuan, "Active clamping circuit with status feedback for series-connected hv-igbts," *IEEE Transactions on Industry Applications*, vol. 50, no. 5, pp. 3579 – 3590, 2014.

[25] T. Lu, Z. Zhao, S. Ji, H. Yu, and L. Yuan, "Active clamping circuit with status feedback for series-connected hv-igbts," *IEEE Transactions on Industry Applications*, vol. 50, no. 5, pp. 3579–3590, Sept. 2014.

[26] L. Yang, P. Fu, X. Yao, and J. Wang, "A module based self-balanced series connection for igbt," in *2014 IEEE Energy Conversion Congress and Exposition (ECCE)*, 2014.

[27] L. Yue and X. Yao, "Implementation of a self-balancing control for series igbts," in *2018 IEEE Energy Conversion Congress and Expo (ECCE)*, Portland, OR, USA, 2018.

[28] S. Jeong and M. Park, "The analysis and compensation of dead-time effects in pwm inverters," *IEEE Transactions on Industrial Electronics*, vol. 38, no. 2, pp. 108 – 114, 1991.